Catalysis Today 148 (2009) 153–159

Contents lists available at ScienceDirect

Catalysis Today

journal homepage: www.elsevier.com/locate/cattod

# Catalytic behavior of CoMo/ZSM5 catalysts for $CS_2$ conversion

G. Espinosa *, J.M. Dominguez, L. Diaz, C. Angeles

*Instituto Mexicano del Petróleo, Programa de Ingeniería Molecular, Eje Central Lázaro Cárdenas 152, 07730 Mexico, D.F., Mexico*

ARTICLE INFO

*Article history:*
Available online 1 May 2009

*Keywords:*
Zeolites
Hydrocarbon reactions
Metallic catalysts

ABSTRACT

Catalysts based upon ZSM-5 zeolites ($SiO_2/Al_2O_3$ molar ratio of 30 and 150) were synthesized and tested for the carbon disulfide ($CS_2$) conversion. First, the zeolites were shaped in pellets using alumina (20 wt%) as binder. The pellets containing ZSM5 ($SiO_2/Al_2O_3 = 30$) were exchanged with $Co^{2+}$. Afterwards, this material and the other one, having the zeolite with $SiO_2/Al_2O_3$ ratio of 150, were co-impregnated with Mo and Co salts. The structural variations were explored by means of X-Ray Diffraction. The progressive reduction of the metal phases was studied by Thermal Programmed Reduction (TPR); the acidity distribution was evaluated by FTIR-pyridine adsorption and the aggregation state of the crystalline phases was characterized by High Resolution Transmission Electron Microscopy (HRTEM) and EDS. The catalytic properties were evaluated in a fixed bed reactor at 350 °C, $P = 20$ kg/cm$^2$ with a $H_2/CS_2$ molar ratio equal to 2. The results suggest a hindering of catalytic activity by the metal phase, which is deposited either on the alumina or over the external surface of the zeolite crystallites.



## 1. Introduction

Hydrogen sulfide ($H_2S$) is an acid gas often considered as a noxious contaminant that is currently found in petroleum and gas resources worldwide. This acid gas may be an important part of the low-grade natural gas reservoirs, which have a variable proportion of $H_2S$ that ranges from a few percentage up to about 90% $H_2S$ [1]. For this reason the low grade gas reservoirs may become economically unpractical [2]. Furthermore, an important part of the global gas reserve is located in remote sites that have a limited horizon of production and also have a significant concentration of $H_2S$, which does not justify the installation of conventional sweetening units. On the other hand, the acid gas ($H_2S$) is found in the petroleum refining and gas processing industries as a by product of the hydrodesulfurization process (HDS), which is widely used for removing sulfur from hydrocarbons. The resulting $H_2S$ fraction is currently treated in the sulfur recovery units by means of the Claus process, a multi-reactor system for the progressive catalytic oxidation of $H_2S$, where two parts of $H_2S$ and one part of $SO_2$ are obtained first in a high temperature thermal unit and this composition reacts further along a catalytic reaction train of 1 to 3 reactors, to produce elemental sulfur and water, i.e., $2H_2S + SO_2 \rightarrow 3S + 2H_2O$; however, this process leaves commonly 1–3% of residual $H_2S$, which must be processed further by a tail gas process (TGP) like the Scott or Super Claus processes [3,4], i.e., $H_2S + {}^1/_2O_2 \rightarrow S + H_2O$. Nowadays the global $H_2S$ removal that is achieved in a typical Claus unit with 3 catalytic converters and a TGP process is about 99.7%. Alternatively, recent developments [5] consider $H_2S$ as an asset rather than a nuisance, as it can be a valuable source of hydrogen and also it may be a reactant for performing the methane reforming to produce valuable products, i.e., $CH_4 + 2H_2S \rightarrow CS_2 + 4H_2$; this reaction yields hydrogen and carbon disulfide ($CS_2$), in particular $CS_2$ is a chemical precursor for the synthesis of cellophane, thiocarbamates and sulfuric acid, among other products. In turn, the catalytic hydroconversion of $CS_2$ has a potential interest for obtaining liquid hydrocarbons like light naphtha [5], by means of the following reaction: $CS_2 + 3H_2 \rightarrow -[CH_2]- + 2H_2S$. The $H_2S$ may be recycled for alternative uses.

Although this is an important route for the use of $H_2S$, the reports are rather scarce, but previous works claim the use of MFI type zeolites as a catalyst for the conversion of $CS_2$ [6–8], which use the shape selective properties of HZSM5 [9]. On the other hand, the CoMoS and NiMoS metallic phases supported on alumina have been widely used for HDS of gasoil [10–12]; thus, in the present work it is of interest to prove these concepts by exploring the use of MFI type zeolites (i.e., $SiO_2/Al_2O_3$ molar ratios of 30 and 150) as the supports of CoMo metallic phases, for the $CS_2$ conversion reaction. In particular, these bifunctional catalysts have not been reported as catalysts for promoting this reaction, which could open potential ways of extending the alternative use of the acid gas ($H_2S$).

* Corresponding author.
*E-mail address:* gaespino@imp.mx (G. Espinosa).

0920-5861/$ – see front matter © 2009 Elsevier B.V. All rights reserved.
doi:10.1016/j.cattod.2009.03.029

## 2. Experimental

### 2.1. Catalysts preparation

The ZSM5 zeolites with $SiO_2/Al_2O_3$ molar ratio of 30 and 150 (Zeolyst International) were exchanged with $NH_4^+$ and then were calcined at 550 °C during 6 h, to obtain the zeolitic acidic form. The samples were pelletized with the use of boehmite Catapal B as a binder. The cylindrical pellets containing 80 wt % zeolite, were calcined at 550 °C for 6 h. The catalyst containing ZSM5 with a $SiO_2/Al_2O_3$ molar ratio of 30 was labeled as ZS-1, and the other material containing the zeolite of 150 was named as ZS-2. The ZS-1 pellets were exchanged with $Co^{2+}$, using a solution of 100 ml/g of 0.1 M $Co(NO_3)_2$. The procedure was carried out under reflux at 80 °C during 6 h; afterwards, the samples were filtrated and rinsed with deionized water. The solid obtained was named CZS-1. Afterwards, bifunctional catalysts were prepared by incipient co-impregnation over CZS-1 and ZS-2 pellets, using the proper volumes of aqueous solutions of 0.07 M ammonium heptamolybdate and 0.6 M cobalt nitrate. The two impregnated materials were dried at 120 °C overnight and then, were calcined at 500 °C during 6 h. The chemical composition of the catalysts was determined by Atomic Absorption. The CZS-1 supported CoMo catalyst is labeled CMZS-1, while another catalyst prepared with the ZS-2 support is labeled as CMZS-2 catalyst.

### 2.2. Characterization

The aggregation states of the crystalline phases were characterized by X-Ray Diffraction, using a Bruker diffractometer fitted with a Cu Kα radiation source. The XRD patterns were recorded in air atmosphere, following the reduction treatment of samples CMZS-1 and CZS-1, at 450 °C under hydrogen flow.

A series of TPR experiments were carried out using an Altamira Instruments II, in which the powder samples were dried at 100 °C during 1 h, then the temperature was lowered down to room temperature, followed by reduction under $H_2$ (10 vol% in Argon) with a heating ramp of 5 °C/min, until 850 °C.

The surface acid properties of the catalysts were monitored by Fourier Transform Infrared Spectroscopy (FTIR) of adsorbed pyridine, using a spectrometer Nicolet, model 710. For this, self-supported wafers were prepared from the powder samples, which were mounted on a Pyrex cell fitted with $CaF_2$ windows. The samples were first purged during 1 h at 400 °C, and then the temperature was decreased at 25 °C, before introducing pyridine during 30 min under a pressure of a few torr. The FTIR spectra were obtained after out-gassing the samples at temperature steps of 200, 300, 400 and 500 °C.

The catalysts were studied by High Resolution Transmission Electron Microscopy (HRTEM) using a JEOL (200 Kv) 2200 FS microscope. The samples were mounted onto holey carbon coated copper grids after a dehydration treatment overnight at 573 K. Also, the chemical analysis by Energy Dispersive Spectrometry (EDS) was performed in the microscope, which led to determine the compositional features of the metal particles that formed in the CMZS-1 and CZS-1 catalysts that were reduced in hydrogen.

### 2.3. Catalytic properties

A fixed bed reactor was used for carrying out the reaction between $CS_2$ and hydrogen. This system was coupled to a gas chromatograph (Varian 3400CX) fitted with a TCD detector, which was used for the analysis on-line of the gaseous products. The liquid products were collected in a cold trap and were analyzed in another gas chromatograph (i.e., a Varian CP3800) fitted with a FID detector (DHA method). The sulfur compounds in the liquid phase were analyzed by means of a GC Agilent 6890N fitted with a MS detector.

**Table 1**
Materials and catalysts composition.

| Samples | $SiO_2/Al_2O_3$ ZSM-5 (raw) | Co (wt%) | Mo (wt%) | Bronsted acid sites** (μmol/g cat) |
|---|---|---|---|---|
| ZSM5-30* | 30 | 0 | 0 | 163 |
| ZSM5-150* | 150 | 0 | 0 | 18 |
| ZS-1 | 30 | 0 | 0 | 24 |
| ZS-2 | 150 | 0 | 0 | – |
| CZS-1 | 30 | 0.27 | 0 | – |
| CMZS-1 | 30 | 1.04 | 4.17 | – |
| CMZS-2 | 150 | 0.65 | 1.95 | – |

* Pure samples.
** Sites at 400 °C.

Carbon disulfide (Aldrich, 98% purity) was fed to the reactor by means a pump (Optos 1LM-3/32). The cylindrical pellets ($\Phi$ = 1 mm) were charged into the reactor and were mixed with silicon carbide powder (40–60 mesh), with the purpose of limiting any diffusion effects.

The molar ratio of the reactant gases (i.e., $H_2/CS_2$) was equal to 2 and the pressure was set at 20 kg/cm$^2$, while the temperatures varied between 350 °C and 500 °C. The $CS_2$ contents into gas and liquid products were obtained in order to achieve the total mass $CS_2$ at the exit ($M_{CS2exit}$). The $CS_2$ mass at the entrance ($M_{CS2feed}$) was adjusted by the pump. Then the conversion was calculated as follows:

$$\%X = (M_{CS2feed} - M_{CS2exit}) \times \frac{100}{M_{CS2feed}}.$$

The reduction of the metallic phase was carried out *in situ* before the catalytic tests, at 450 °C, under pure hydrogen flow, during 6 h. This temperature was chosen because there is previous report [13] indicating that above 500 °C, the reduction of molybdenum species could cause a decrease of the catalytic activity. The contact of the feed gas ($H_2/CS_2$) at high temperatures with a CoMo phase leads to a direct sulfidation to form CoMoS species, and this could be the main active phase for the $CS_2$ conversion.

## 3. Results and discussion

The composition of the catalysts based upon ZSM5 zeolites and metals (Co, Mo) is summarized in Table 1. Also, this table shows the number of Brönsted acid sites, which were measured by FTIR/pyridine adsorption at 400 °C.

Also, Fig. 1 shows the XRD patterns corresponding to ZS-1 and CMZS-1, which illustrate the typical structural features of MFI

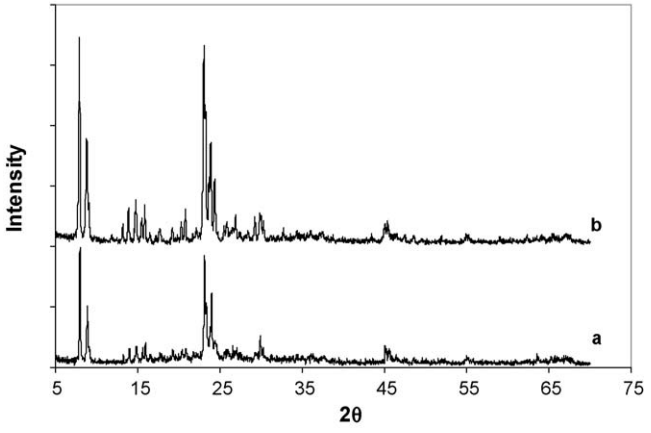


**Fig. 1.** XRD patterns of (A) CMZS-1 and (B) ZS-1.

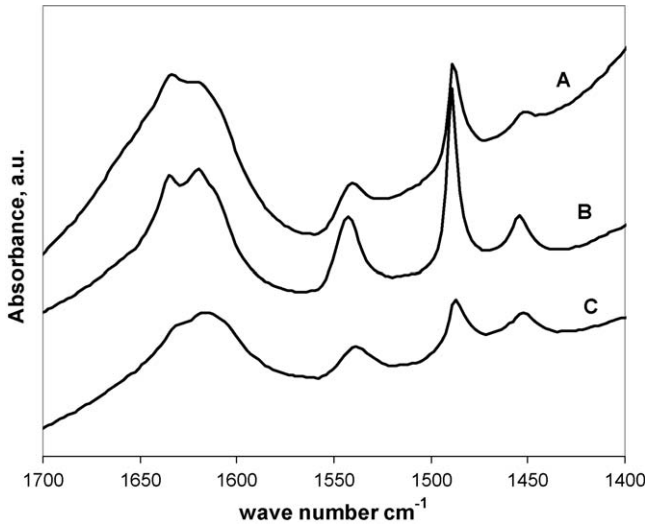


**Fig. 2.** FTIR/pyridine spectra of the materials: (A) pure ZSM-5 with $SiO_2/Al_2O_3$ of 150; (B) pure ZSM-5 with $SiO_2/Al_2O_3$ of 30, and (C) ZS-1 pellets.

zeolites, however the XRD peaks corresponding to the oxide and metallic phases that are present in the CMZS-1 catalysts do not appear because their concentration is very low and their particle size is very small.

For comparison, Table 1 includes the data of pure zeolites having a $SiO_2/Al_2O_3$ ratio of 30; for this case the population of Bronsted acid type sites is more important, as expected for a zeolite that is richer in aluminum than other materials. The Fig. 2 shows the pyridine adsorption bands over Lewis acid type sites at 400 °C, both for the pure zeolites and those corresponding to catalysts pellets of ZS-1, which were prepared from ZSM5 with a $SiO_2/Al_2O_3$ ratio of 30. The IR absorption band appearing at ~1542 $cm^{-1}$ is assigned to the protonation of pyridine by Bronsted acid type sites belonging to the zeolites, while the band appearing at ~1453 $cm^{-1}$ is assigned to the pyridine adsorbed on Lewis acid type sites. These results indicate that the alumina contained in the catalysts ZS-1 might hinder the pyridine adsorption on ZSM5, as if many sites were not accessible to pyridine under the actual conditions. Similarly, the spectra of ZS-2 (not shown here) show barely any trace of Bronsted acid sites. For this case the catalysts have a very small amount of aluminum, and then, one should expect a very low number of Bronsted acid sites.

The $H_2$-TPR profiles are shown in Fig. 3, where one observes an important peak at 423 °C for the catalyst CMZS-1, which is attributed to the reduction of the species $Mo^{+6}$ to $Mo^{+4}$, from the $MoO_3$ polymeric species [14–17]. In addition, at 489 °C this catalyst shows an important reduction peak that can be assigned to the reduction of the $CoMoO_4$ phase, in agreement with previous reports. This catalyst was prepared by co-impregnation of CZS-1 with Co and Mo salts. The former exchange of $Co^{2+}$ with the ZSM-5 zeolite cause a wider reduction peak that is centered around 484 °C.

The catalyst CMZS-2 shows a reduction peak at about 514 °C, which may be attributed to the combined phase $CoMoO_4$. Also, at 724 °C there appears a peak that is generally assigned to the reduction of the $Mo^{2+}$ phase to $Mo^0$, this phase does not interact with the metallic cobalt phase [14–17].

The Mo precursor, ammonium heptamolybdate, is a bulky and negatively charged chemical species, which is expected to interact weakly with the zeolite surface, which is more acidic ($SiO_2/Al_2O_3$ = 30) in the conditions of impregnation [18,19]. The weak interaction between the metallic species with the support may be the cause of the temperature shift that was observed in the reduction peak corresponding to the CoMo phase in the CMZS-1

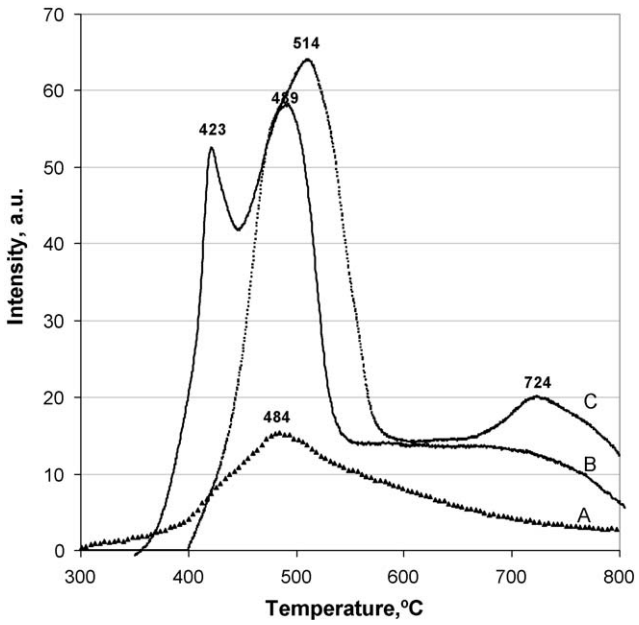


**Fig. 3.** TPR profiles of CoMo species: (A) CZS-1, (B) CMZS-1 and (C) CMZS-2.

catalyst (Fig. 3). The catalyst CMSZ-2, which has a $SiO_2/Al_2O_3$ ratio of 150, shows a reduction peak at 514 °C, which suggests a stronger interaction of the CoMo phase with the zeolite surface.

In order to understand better the interaction between the metallic phases with the support, a study was made on the main structural features of the supported metal particles, by means of High Resolution Transmission Electron Microscopy (HRTEM). Thus, the aggregation state and composition of the metallic phase in the catalysts were studied by HRTEM and Energy Dispersive Spectroscopy (EDS). However, there are scarce references regarding the characterization of zeolites by HRTEM methods, because these materials undergo a rapid structural degradation under the observation conditions in the electron microscope. Thus, in the present case only the samples that were dehydrated at 100 °C and calcined at 550 °C in dry air (only for the sample ZS-1) were studied by the HREM methods and a previous treatment was applied by means of an evacuation overnight before observation. A typical lattice image corresponding to the ZS-1 catalyst is shown in Fig. 4, which corresponds to the <0 1 0> crystal orientation. This image illustrates the structural features of ZSM5, which coincide with the inner pore arrays that are typical of MFI type zeolites, with a pore diameter of 0.57 nm.

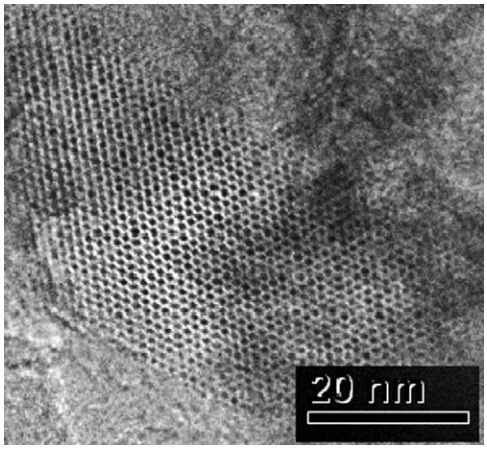


**Fig. 4.** Bright Field HRTEM image of the catalyst ZS-1.

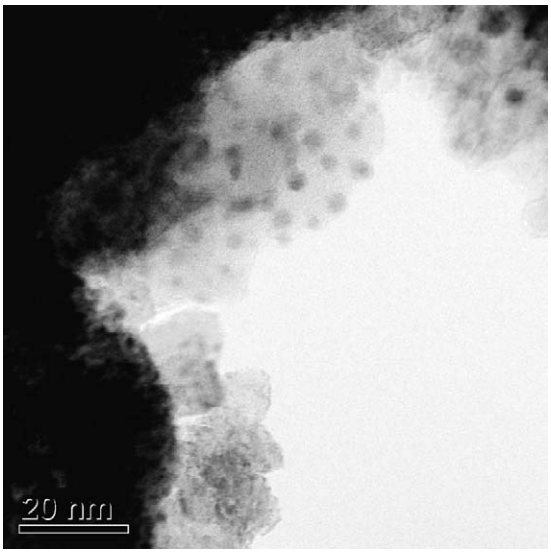


**Fig. 5.** Bright Field Image of the metal particles in the catalyst CMZS-1.

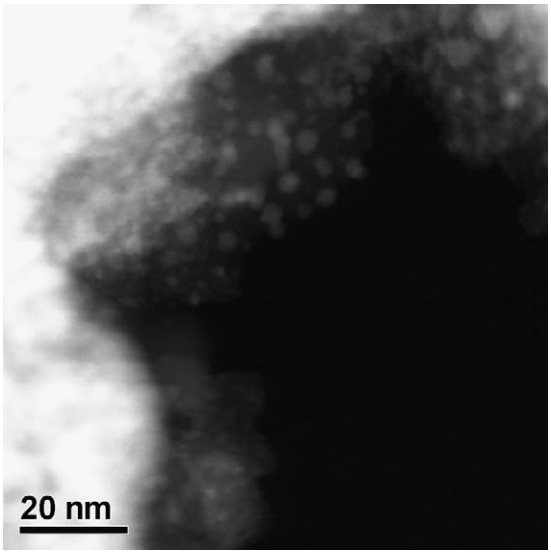


**Fig. 6.** HAAD Image showing the metal particles contrast (bright) in the catalyst CMZS-1. Notice the correspondence with particles in Fig. 5 (one-to-one).

Also, a closer approach to know the main structural features of the metal particles was made by means of the HRTEM-BF and HRTEM-HAAD techniques. Thus, Figs. 5 and 6 illustrate the correspondence between the Bright Field images of metal particles and the HAAD images of the same area, for the catalyst CMZS-1; one observes that most of the metal particles are dispersed over the support and have a particle diameter of about 4 nm. The HAAD image shown in Fig. 6 is a Z-depending contrast, corresponding to the same area, with metal particles showing a bright contrast. The individual particles were analyzed by EDS for determining the chemical composition, as shown in Fig. 7, where the peaks corresponding to Mo-L, Mo–K and Co–L emissions are clearly outlined, together with other peaks that arise from the support material (Al, Si) and the copper grid (Cu). The Mo and Co EDS-peak intensities lead to the relative chemical composition (Table 2), where the composition of four individual metal particles is reported. These results indicate that the metal particles have a bimetallic character with a variable Co/Mo composition (Table 2).

**Table 2**
EDS Analysis for CMZS-1.

| | Point analysis (wt%) | | | |
|---|---|---|---|---|
| Element | 1 | 2 | 3 | 4 |
| Co | 25.23 | 35.10 | 38.14 | 40.10 |
| Mo | 74.77 | 64.90 | 61.86 | 59.90 |

A further study of the metal particles by HRTEM techniques is illustrated by the Fig. 8A and B, where one observes the inner structural features of the small metal particles (arrowed). Fig. 8A shows two particles of about 2.5 nm diameter, which are magnified in Fig. 8B, where one observes the lattice planes in a diamond-like array, though some planes are like weaving along the main directions. A picture illustrating the lattice images observed in the electron microscope is shown in Fig. 9, which corresponds to the body-centered cubic structure projected along [1 0 0] and [1 1 1], respectively, where the second one is the cube diagonal axis, thus the typical diamond array is more apparent when the structure is projected on the (1 1 1) plane. This lattice is bcc, which corresponds to the structure of Mo metal [20], with a Space group I*m*-3*m* (SG No. 229). The cell parameters were determined from the HREM images and were found close to the ideal values, i.e., $a = b = c = 0.314$ nm, $\alpha = 90^{\circ}$. Also, the presence of Co into the metallic particles causes a slight distortion between the Mo planes, as observed in the experimental pictures (Fig. 8A and B).

In contrast to these results, the HREM images of the CZS-1 catalysts (after reduction) do not show the presence of metal particles. These catalysts were prepared by exchanging $Co^{2+}$ ions with the zeolite sites and were reduced under hydrogen, thus the apparent absence of metallic particles on these catalysts lead us to deduce that the metal phase is highly dispersed on the zeolite support, or alternatively, the metal particles could be confined into the zeolite channels system.

The catalytic properties were tested in a fixed bed type reactor and the main results are condensed in Table 3, which illustrates the selectivity patterns of different catalysts and a relative comparison under similar conversion values. A typical run contains some gaseous products like $H_2S$ and Methanethiol (methyl-mercaptan), the latter being obtained more abundantly. Also, several alkyl mercaptans in the liquid phase were detected in the GC Agilent 6890N system coupled to a MS detector. The bi-functional character of CoMo catalysts makes it that catalysts become more active at 350 °C than their ZSM5 zeolite support; thus, in this series

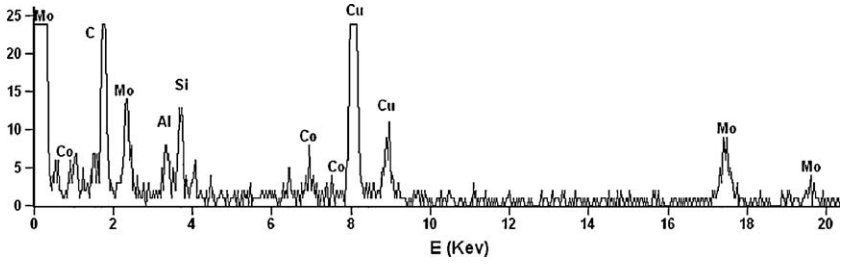


**Fig. 7.** A typical Energy Dispersive Spectrum (EDS) of a single metal particle.

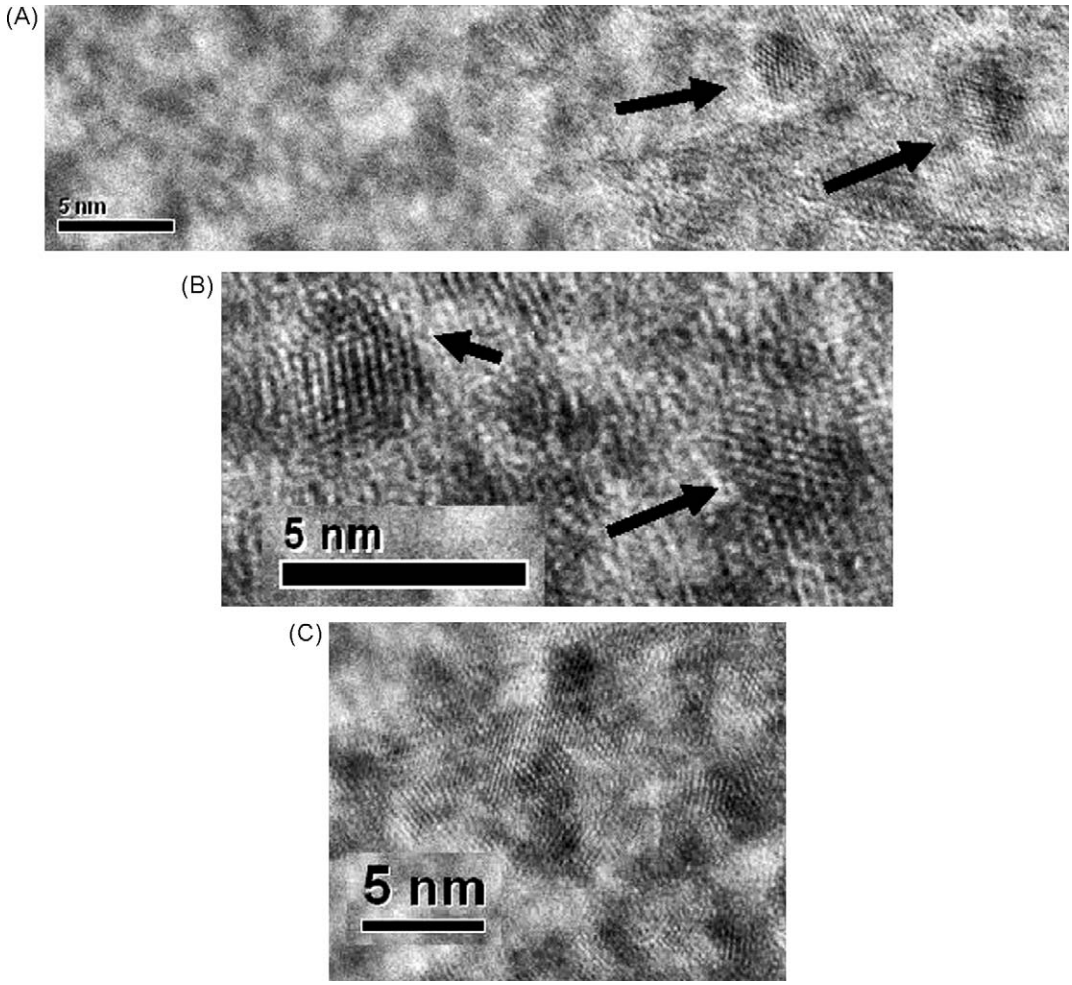


**Fig. 8.** Transmission Electron Microscopy images of supported metal (Co, Mo) particles in the catalysts CMZS-1.

of tests, gaseous products are predominant. The distribution of the hydrocarbon products was plotted against the carbon number (Figs. 10 and 11). The product distribution corresponding to the ZS-1 catalyst (Fig. 10A) contains significant amounts of $C_6$+ hydrocarbons (paraffins, isoparaffins, naphthenes and aromatics). Fig. 10B shows the selectivity for CZS-1, which suggests that the catalysts prepared by ion exchanging $Co^{2+}$ ions produce a higher amount of olefins in the interval $C_4^=$–$C_5^=$. Following this trend, it is observed that the bimetallic phase (CoMo) has a stronger effect on the product selectivity (Fig. 10C), where $C_5$ olefins are the most important products when CMSZ-1 catalyst is used.

On the other hand, the selectivity of the catalyst ZS-2 (Fig. 11A), which contains a lesser amount of acid sites with respect to ZS-1, is very similar to CZS-1, which might indicate that $Co^{2+}$ ions could cause a diminution on the number of surface acid sites of the material ZS-1. Also, it is expected that the selectivity pattern may be strongly affected by the CoMo phase in the ZS-2 type materials, which was verified by the distribution of products that were obtained with the catalyst CMZS-2; in this case there is a preferential formation of $C_4$ and $C_5$ olefins, similar to CMZS-1 (Figs. 10C and 11B).

The HRTEM observations and EDS analysis show that the CoMo species form small metal particles that are deposited outside the zeolitic crystallites in the CMZS-1 catalysts. This result is probably due to the incipient impregnation method, which could lead to an inhomogeneous metal distribution derived from a rather weak interaction between the zeolite and the metal phase, as suggested from the TPR experiments. Then, during the impregnation step the Mo and Co precursors are preferentially deposited on the alumina binder, where there is a stronger interaction and this makes it that during the calcination, reduction and sulfidation, this configuration remains.

Therefore, the $CS_2$ molecules should react more easily on the accessible CoMo phase and the olefins formed might desorb before interacting with the zeolite phase. As it is proposed in other condensation process reports [21], the olefins formation is an intermediary an important step. In order to form the rest of

**Table 3**
Reaction data from catalysts based on Zeolites ZSM-5.

| Catalyst | ZS-1 | CZS-1 | CMZS-1 | ZS-2 | CMZS-2 |
|---|---|---|---|---|---|
| $CS_2$ conv. % | 10.81 | 15.48 | 20.90 | 7.939 | 16.80 |
| $H_2S$* | 74.71 | 71.03 | 75.06 | 75.42 | 67.82 |
| Methylmercaptane* | 1.09 | 4.48 | 2.17 | 2.32 | 1.90 |
| Methane* | 1.14 | 10.75 | 15.90 | 0.58 | 15.35 |
| Liquid fraction** | | | | | |
| Aromatics | 3.95 | 2.19 | 2.55 | 3.11 | 0.42 |
| Isoparaffins | 27.91 | 32.5 | 7.57 | 28.02 | 6.46 |
| Naphthenes | 21.29 | 3.71 | 0.97 | 4.57 | 0.61 |
| Olefins | 2.17 | 46.83 | 69.04 | 38.30 | 88.31 |
| Paraffins | 28.03 | 4.94 | 0.92 | 3.53 | 0.92 |
| Unknown | 16.63 | 4.72 | 14.41 | 5.42 | 2.21 |
| C13+ | 0.02 | 0.75 | 0.0 | 0.1 | 0.0 |

Reaction conditions: $T$ = 350 °C, $P$ = 20 kg/cm$^2$, $H_2/CS_2$ = 2, and LHSV = 1 h$^{-1}$.
* Results obtained from the analysis by TCD of the gaseous fraction.
** Only hydrocarbon from the liquid fraction determined by DHA.

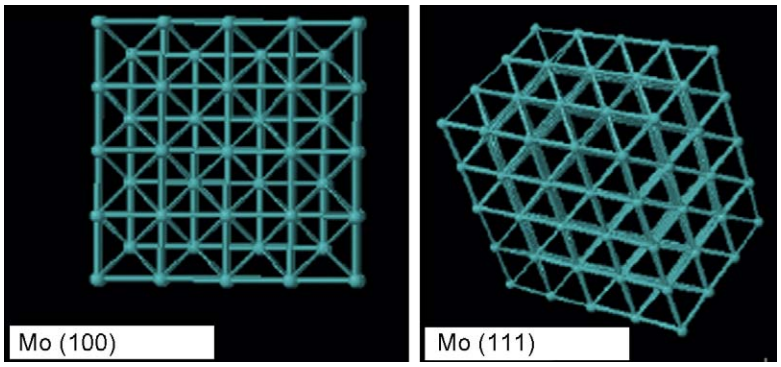


**Fig. 9.** Structural Model for Mo-bcc projected onto (1 0 0) and (1 1 1) planes.

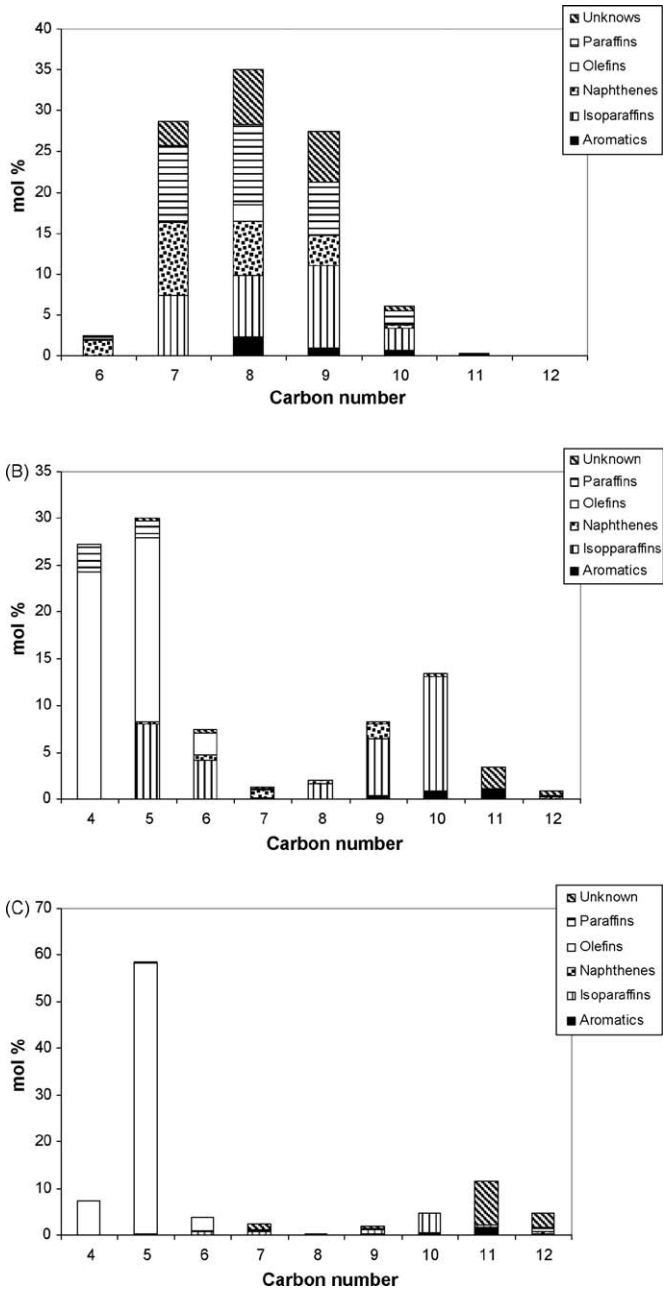


**Fig. 10.** Products distribution obtained at 350 °C, P: 20 kg/cm$^2$, $H_2/CS_2$ = 2, and LHSV = 1 h$^{-1}$ with catalysts prepared from the ZSM5 ($SiO_2/Al_2O_3$ = 30): (A) ZS-1, (B) CZS-1 and (C) CMZS-1.

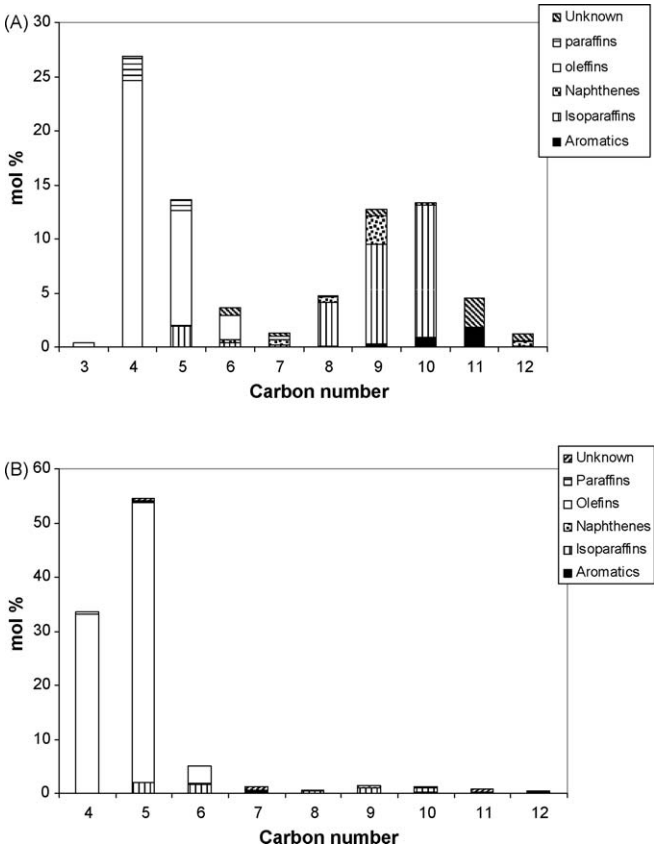


**Fig. 11.** Products distribution obtained at 350 °C, P: 20 kg/cm$^2$, $H_2/CS_2$ = 2, and LHSV = 1 h$^{-1}$ with catalysts prepared from the ZSM5 ($SiO_2/Al_2O_3$ = 150): (A) ZS-2, (B) CMZS-2.

products, for example, isoparaffins, it is required that intermediary olefins react with the acid sites present on the zeolite. In addition, the formation of aromatics and naphtenes requires their access into the channels framework. However, as we deduce from the FTIR study, there are acid sites in the zeolite which are relatively inaccessible both to the reactant and intermediary molecules. For promote the entrance of molecules should be necessary increase the temperature, but at such condition, the $CS_2$ would be quickly transformed in gaseous products in presence of the CoMo phase.

## 4. Conclusions

The $CS_2$ hydrogenation was carried out using catalysts based upon the main properties of ZSM5 type zeolites. The ionic exchange of $Co^{2+}$ with these zeolytic materials seems to provoke a decrease of

the total number of acid sites (Bronsted type) and, consequently, the catalytic behavior of the pure zeolytic phase is modified. The catalyst based upon ZSM5, which has a $SiO_2/Al_2O_3$ ratio of 150 shows a similar catalytic selectivity with respect to CZS-1.

The metallic phase in these catalysts strongly affects the catalytic behavior of the original zeolites, thus suggesting that in these systems the catalytic properties are hindered or modified negatively by the metallic phases.

## References

[1] H.S. Meyer, Volume and distribution of sub-quality natural gas in the U.S., Gas TIPS, GTI web: <http://www.gri.org/pub/content/feb/20000224/110827/gtwn00b.html>.
[2] R.H. Hugman, E.H. Vidas, P.S. Springer, Chemical composition of discovered and undiscovered natural gas in the U.S. 1993 Update, GRI-93/0456.
[3] J.A. Lagas, J. borsn¿boom, P.H. Berben, in: Proceedings of the 38th Annual Laurance Reid Gas Conditioning Conference, March 7–9, 1988.
[4] P.F.M.T. van Nisselroy, J.A. Lagas, Catal. Today 16 (1993) 263–271.
[5] E.J. Erekson, F.Q. Miao, Quarterly progress report for the period Jan–March 1994, U.S. DOE, DOE/PC/92114-T3, June 1994.
[6] C.D. Chang, US Patent 4,543,434 (1985).
[7] R.E. Palermo, S. Han, US Patent 4,864,073 (1989), Lawrenceville, NJ.
[8] C.D. Chang, W.H. Lang, US Patent 4,480,143 (1984).
[9] C.P. Nicolaides, N.P. Sincadu, M.S. Scurrell, Catal. Today 71 (2002) 429–435.
[10] X. Song, A. Sayari, Energ. Fuel 10 (1996) 561–565.
[11] T. Fujikawa, Catal. Surv. Asia 10 (2006) 89–97.
[12] S. Chaturvedi, J.A. Rodrigueza, J.L. Brito, Catal. Lett. 51 (1998) 85–93.
[13] P. Wehrer, L. Hilaire, E. Petit, Appl. Catal. A: Gen. 273 (2004) 249–258.
[14] J.L. Brito, J. Therm. Anal. 49 (1997) 535–540.
[15] J. Sarrın, O. Noguera, H. Royo, M.J. Pérez Zurita, C. Scott, M.R. Goldwasser, J. Goldwasser, M. Houalla, J. Mol. Catal. A: Chem. 144 (1999) 441–450.
[16] Li Wei, Sara Y. Yu, George D. Meitzner, E. Iglesia, J. Phys. Chem. B 105 (2001) 1176–1184.
[17] O.G. Marin Flores, Su Ha, Appl. Catal. A: Gen. 352 (2009) 124–132.
[18] J.P. Tessonnier, B. Louis, S. Rigolet, M.J. Ledoux, C. Pham-Huu, Appl. Catal. A: Gen. 336 (2008) 79–88.
[19] P.L. Tan, Y.L. Leung, S.Y. Lai, C.T. Au, Appl. Catal. A: Gen. 228 (2002) 115–125.
[20] R.G. Ross, W. Hume-Rothery, J. Less-Common Met. 5 (1963) 258.
[21] E. Iglesia, S.L. Soled, J.E. Baumgartner, S.C. Reyes, J. Catal. 153 (1995) 108.